AJNR

MRI-Based Prediction of Clinical Improvement Following Ventricular Shunt Placement for Normal Pressure Hydrocephalus (NPH): Development and Evaluation of an Integrated Multi-Sequence Machine Learning Algorithm

Owen P. Leary, Zhusi Zhong, Lulu Bi, Zhicheng Jiao, Yu-Wei Dai, Kevin Ma, Shanzeh Sayied, Daniel Kargilis, Maliha Imami, Lin-Mei Zhao, Xue Feng, Gerald Riccardello, Scott Collins, Konstantina Svokos, Abhay Moghekar, Li Yang, Harrison Bai, Petra M. Klinge and Jerrold L. Boxerman

ORIGINAL RESEARCH

MRI-Based Prediction of Clinical Improvement Following Ventricular Shunt Placement for Normal Pressure Hydrocephalus (NPH): Development and Evaluation of an Integrated Multi-Sequence Machine Learning Algorithm

Owen P. Leary BS*, Zhusi Zhong BS*, Lulu Bi BS, Zhicheng Jiao PhD, Yu-Wei Dai MD, Kevin Ma BS, Shanzeh Sayied BS, Daniel Kargilis BS, Maliha Imami BS, Lin-Mei Zhao MD PhD, Xue Feng PhD, Gerald Riccardello MD, Scott Collins RT(R)(CT), Konstantina Svokos DO MS, Abhay Moghekar MD, Li Yang MD PhD, Harrison Bai MD MS, Petra M. Klinge MD PhD, Jerrold L. Boxerman MD PhD

ABSTRACT

BACKGROUND AND PURPOSE: Symptoms of normal pressure hydrocephalus (NPH) are sometimes refractory to shunt placement, with limited ability to predict improvement for individual patients. We evaluated an MRI-based artificial intelligence method to predict post-shunt NPH symptom improvement.

MATERIALS AND METHODS: NPH patients who underwent magnetic resonance imaging (MRI) prior to shunt placement at a single center (2014-2021) were identified. Twelve-month post-shunt improvement in modified Rankin Scale (mRS), incontinence, gait, and cognition were retrospectively abstracted from clinical documentation. 3D deep residual neural networks were built on skull stripped T2-weighted and fluid attenuated inversion recovery (FLAIR) images. Predictions based on both sequences were fused by additional network layers. Patients from 2014-2019 were used for parameter optimization, while those from 2020-2021 were used for testing. Models were validated on an external validation dataset from a second institution (n=33).

RESULTS: Of 249 patients, n=201 and n=185 were included in the T2-based and FLAIR-based models according to imaging availability. The combination of T2-weighted and FLAIR sequences offered the best performance in mRS and gait improvement predictions relative to models trained on imaging acquired using only one sequence, with AUROC values of 0.7395 [0.5765-0.9024] for mRS and 0.8816 [0.8030-0.9602] for gait. For urinary incontinence and cognition, combined model performances on predicting outcomes were similar to FLAIR-only performance, with AUROC values of 0.7874 [0.6845-0.8903] and 0.7230 [0.5600-0.8859].

CONCLUSIONS: Application of a combined algorithm using both T2-weighted and FLAIR sequences offered the best image-based prediction of post-shunt symptom improvement, particularly for gait and overall function in terms of mRS.

ABBREVIATIONS: NPH = normal pressure hydrocephalus; iNPH = idiopathic NPH; sNPH = secondary NPH; AI = artificial intelligence; ML = machine learning; CSF = cerebrospinal fluid; AUROC = area under the receiver operating characteristic; FLAIR = fluid attenuated inversion recovery; BMI = body mass index; CCI = Charlson Comorbidity Index; SD = standard deviation; IQR = interquartile range

SUMMARY SECTION

PREVIOUS LITERATURE: Prior literature has highlighted multiple imaging-based metrics on computed tomography and MRI (e.g., DESH score) which can be useful in diagnosis and outcome prediction of normal pressure hydrocephalus, a neurological disorder defined by a triad of symptoms including gait abnormality, urinary dysfunction, and cognitive impairment. Prediction of improvement following shunt placement surgery remains a challenge, impeding optimal clinical decision-making. We applied artificial intelligence approaches to automatically extract radiomic features from multiple MRI sequences (T2-weighted and FLAIR) acquired preoperatively

from a single-center cohort of patients with NPH and evaluated the performance of models trained to predict function and symptom improvements postoperatively.

KEY FINDINGS: AI algorithms leveraging combined imaging features from preoperative T2-weighted and FLAIR sequences were generally more predictive of postoperative shunt outcome in NPH than models built using one of these sequences. Models performed best for prediction of gait and incontinence improvement, and slightly worse for overall function and cognition.

KNOWLEDGE ADVANCEMENT: We demonstrate implementation of an analytic pipeline for automated radiomic feature extraction from multiple MRI sequences and layered integration of those data to optimize and evaluate prognostic models for normal pressure hydrocephalus, a complex and poorly understood neurologic disorder with defined symptoms and treatment options.

INTRODUCTION

Normal pressure hydrocephalus (NPH) is a progressive neurological disorder characterized by a diagnostic triad of presenting symptoms, including gait instability, urinary incontinence, and cognitive impairment.[1-3] Etiologically, NPH is understood as a form of communicating hydrocephalus which may result from impaired cerebrospinal fluid (CSF) clearance and re-absorbance in the brain.[3, 4] While difficult to diagnose and most frequently idiopathic (iNPH),[5] NPH can also occur secondary to other conditions which influence intracranial CSF dynamics including traumatic brain injury, meningitis, stroke, hemorrhage, or brain tumor (sNPH).[6] The mainstay of treatment for NPH is surgical placement of a ventricular shunt, which drains CSF from the cerebral ventricles to the peritoneal (ventriculoperitoneal) or less commonly the pleural (ventriculopleural) space.[2, 7, 8]

While considered an effective treatment strategy for many patients, symptoms of NPH are sometimes refractory to shunt surgery, with 15-30% of patients experiencing little improvement across symptom domains.[2] Further, traditional methods of simulating CSF drainage, such as high volume lumbar tap test or CSF dynamic testing, have failed to reliably predict which individuals are most likely to benefit from shunting, with negative predictive values of ≤50%.[9-12] While some evidence supports the utility of comorbidity status and other clinical variables in predicting outcome of shunt surgery, models based on comorbidity status alone do not markedly advance clinical decision making capacity.[13-15] Furthermore, imaging biomarkers derived from single-modality imaging (e.g., T2-weighted MRI alone) have failed to significantly improve the overall ability to predict patient outcome.[3, 16, 17]

With artificial intelligence (AI) models increasingly applied to prognostication, there is new opportunity to leverage information drawn from multiple MRI sequences available upon baseline neuroimaging in NPH. While of limited utility in isolation, MRI-derived markers combined into a unified model could advance NPH diagnosis and decision-making.[11, 16-18] In the present study, we hypothesized that AI driven models trained on MRI sequences sensitive to both structural and CSF distribution parameters may predict clinical benefit following shunting for NPH, and that models using multi-sequence information may be the best performing.

MATERIALS AND METHODS

Primary Clinical Dataset

This section may be divided into subsections if it facilitates reading the paper. The research design, patients/subjects, material used, means of confirming diagnoses, and statistical methods should be included. Do not include manufacturer's names unless the specific product is important to the procedures performed. When appropriate, indicate that approval was obtained from the institution's review board. Indicate that informed consent has been obtained from patients who participated in clinical investigations.

In animal experimentation, acknowledge that National Institutes of Health or equivalent guidelines were followed. If there is a sponsoring company, include at the end of this section what input that company had in the formulation of the paper.

The primary dataset included 249 consecutive patients who underwent ventricular shunting for clinical diagnosis of NPH were retrospectively identified from a single institutional cohort (Rhode Island Hospital, Providence RI). 212 patients (85.1%) were diagnosed with iNPH and 37 patients (14.9%) had sNPH. All were treated by one of two neurosurgeons (P.M.K. and K.S.) from 2015-2021. Clinical data were abstracted from recorded clinical documentation by trained research staff. Baseline characteristics including comorbidity status as quantified in the Charlson Comorbidity Index (CCI) were also obtained.[14] Postoperatively, 226 patients (90.8%) returned to clinic at 3-month follow-up and 175 (70.3%) returned for 12-month follow-up. For outcome analysis, 12-month follow-up was preferentially selected whenever available, however if 12-month follow-up was not available 3 month follow-up was utilized for evaluation of the symptom improvement endpoints.

MRI sequences of interest included T2-weighted and fluid attenuated inversion recovery (FLAIR), selected based on availability as part of routine diagnostic MRI acquired during clinical work-up at our center and the hypothesis that these sequences may provide complementary information about underlying disease features (**Figure 1**). 201 patients (80.7%) had preoperative imaging (i.e., T2-weighted

or FLAIR) available for inclusion. Due to lacking imaging and/or follow-up data, 48/249 patients were excluded from the FLAIR-based analysis, and 64/249 patients were excluded from the T2 and T2+FLAIR analyses. Most scans were acquired at a single academic center using a uniform image acquisition protocol, using either a 1.5T or 3.0T magnet, though a minority of cases were captured at outside centers. The acquisition protocols on both scanners were the same except that the slice thickness was 5mm for the 1.5T and 4mm for 3.0T, which is accounted for by preprocessing methods described subsequently. No notable changes in NPH referral processes occurred during the study inclusion period (2015–2021). Accordingly, baseline MRI data from included patients and separated into training and testing sets based on date (approximate 7:3 ratio).
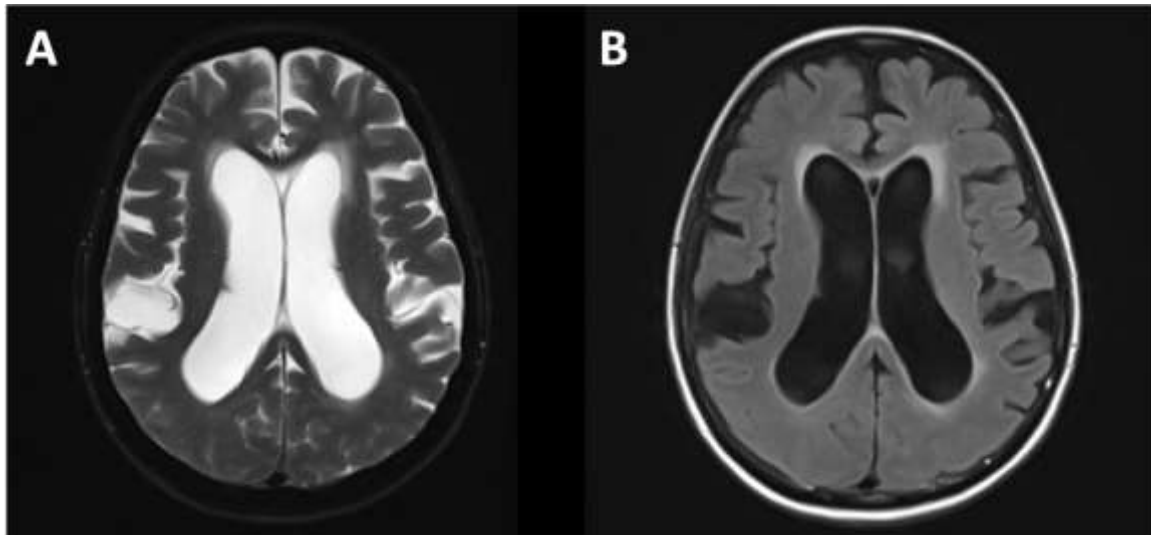
FIG 1. Exemplary axial images fromT2-weighted and FLAIR sequences of an included patient.

Gait and urinary incontinence scores were estimated using previously reported 8- and 6- point symptom scales, respectively.[1, 2] For the gait scale: 1= normal; 2= slight disturbance of tandem walk and turning; 3= wide-based gait with sway; 4= tendency to fall, with foot corrections; 5= walking with cane; 6= bi-manual support; 7= aided by another person; 8= wheelchair-bound. For the incontinence scale: 1= normal; 2= urgency without incontinence; 3= infrequent incontinence; 4= frequent incontinence; 5= complete bladder incontinence; 6= bladder/bowel incontinence. Cognitive impairment was evaluated as present or absent based on patient report and clinician impression. In addition, global functional disability was estimated retrospectively using modified Rankin Scale (mRS).[19] All of these metrics were estimated based on descriptive reports of patient reported symptoms and examination findings in the history and exam sections of baseline and follow-up clinical notes by the two treating surgeons – whenever ambiguity existed between two levels of a given score, the lesser of the two was selected. Improvements in gait, incontinence, and mRS were defined by ≥1 point improvement and improvement in cognition was defined by the patient's and clinician's impression. Binarized clinical endpoints (improved vs. not improved) in each symptom domain and mRS were recorded at 3-months and 12-months postoperatively. Institutional review board (IRB) authorization was obtained for chart and imaging review (#1345067).

External Validation Dataset

To assess generalizability of findings to external NPH cohorts, we obtained an external validation dataset comprising 33 shunted NPH patients with complete follow-up data treated at a second institution within the same period (Johns Hopkins Hospital). The external validation dataset comprised a non-consecutive convenience sample of patients with sufficient follow-up and imaging data from the same treatment period. Imaging sequences and acquisition protocols were generally the same as described above (1.5T or 3.0T magnet with variable slice thickness, but pre-processed uniformly prior to subsequent feature extraction).

Preprocessing

All the FLAIR and T2-weighted images were preprocessed according to the pipeline demonstrated in **Figure 2**. The OncoAI algorithm first registers FLAIR and T2-weighted sequences to a standard template, performs brain extraction, concatenates all sequences, deploys the pre-trained segmentation to obtain the final label map, warps labels back to the original space, and performs limited, stereotyped post-processing.[20] For each study with multiple sequences, the algorithm first parses all series, skips localizer and calibration images, co-

registers all series to a standard template, and resamples to 1x1x1 mm^3 voxel size. Then, the algorithm finds the series that has the largest coverage and runs an AI-based brain segmentation model to extract the brain and warps the brain mask back to each series. The brain space was parcellated from the skull ("skull stripping") and centered within the volume, followed by automated segmentation of intracranial tissue structures (**Figure 2**). MRI images were re-sized to 256x256x64 pixels for the deep neural network. Range scaling normalization was then applied based on intensity value distribution.
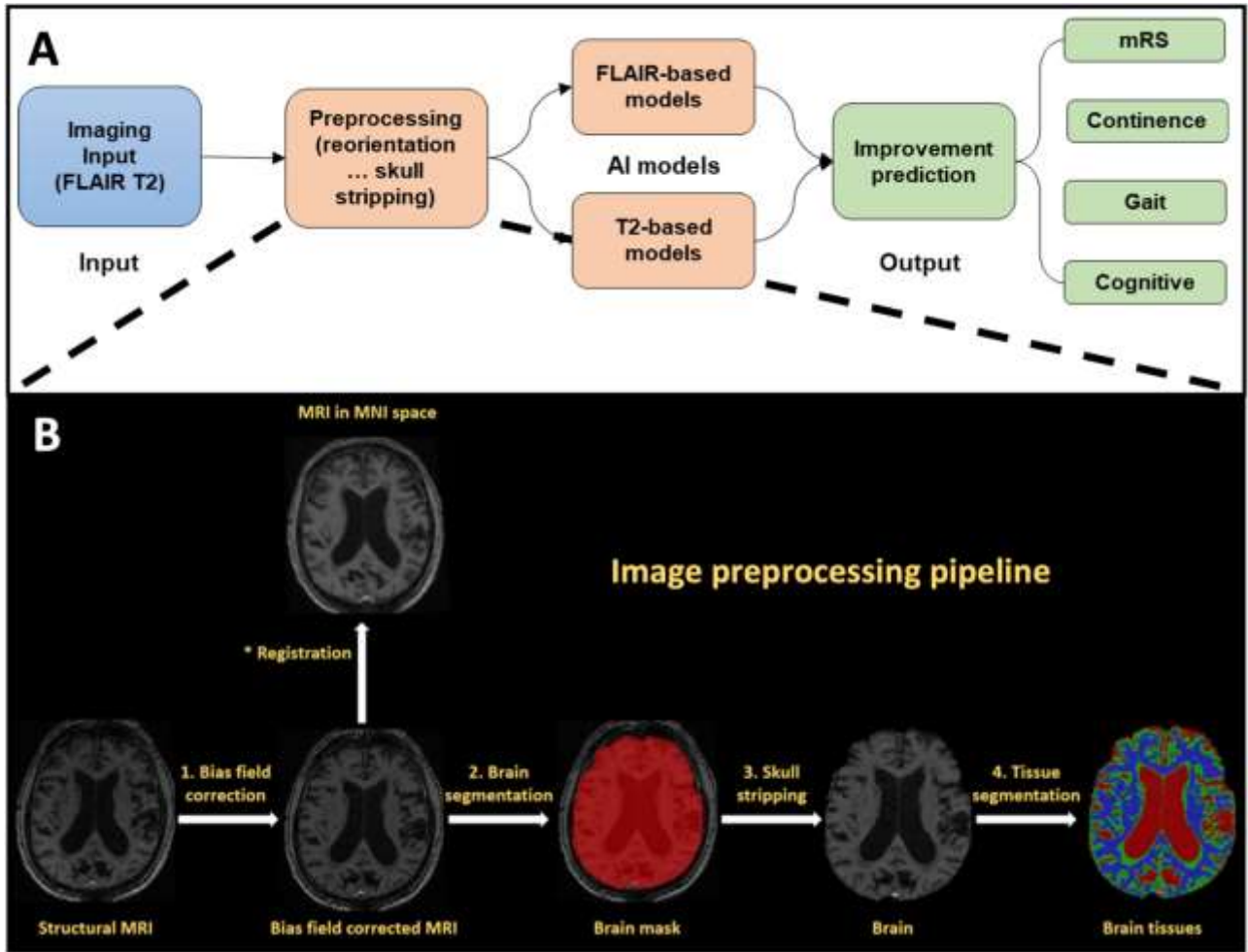
FIG 2. Our AI pipeline for training an outcome prediction model on shunted NPH baseline MRI dataset.

Deep Feature Learning

3D deep residual neural network models were separately built on T2-weighted and FLAIR images for each binary clinical improvement endpoint (i.e. "improved" vs. "not improved" in gait, incontinence, cognition and mRS). We used 3D ResNet-50 as the single modality deep feature extraction model (**Figure 3**). Each block of ResNet-50 is a combination of 3 deep layers with different convolution parameters, in which every 2 residual layers are inserted within this 3-layer bottleneck block, including a total of fifty 3D residual layers. After an average pooling layer, the 2048-dimensional image features extracted by ResNet-50 were used to predict classification probability, constructing a classifier with 3 linear layers with ReLU and Dropout. The numbers of hidden nodes in linear layers were 2048, 2048 and 1024. This pipeline was used for training both the T2- and FLAIR- based models. By contrast, the models trained on both FLAIR and T2-weighted sequences were fused by additional network layers to obtain combined results accounting for both sequences (**Figure 4**). The features of FLAIR and T2-weighted sequences were extracted by two independent deep residual networks, and the two 2048-dimensional features were fused by cascading and passing the classifier to obtain the multi-modality classification probability.

FIG 3. Structure of ResNet50 network

FIG 4. Fusion prediction model with ResNet50 models for integrating information from multiple imaging sequences.

Clinical improvement prediction

We use the cross-entropy loss function during model training. The classification probability estimates the soft target by the SoftMax function, and cross-entropy loss calculates the loss between the soft target and the ground-truth label to learn model parameters:

$$L(y, z) = \sum_{i=0}^{M} -y_i \log(\frac{z_i}{\sum_j \exp(z_j)})$$

In this function, M is the total number of classes (e.g., M=2 when for binary outcome prediction). The variable y_i is a vector representing the ground-truth label of the training set as 1 and all other elements as 0; z_j is the logit which is the output of the last layer for the j-th class of the model. The weight of the model is updated via adaptive moment estimation with weight decay, in which the optimizer calculates the adaptive learning rates of every parameter. The learning rate and weight decay coefficient were set to 0.001. We ran each method for 60 epochs and collected the highest average accuracy per run. The fused (T2+FLAIR) model was then initialized with a model trained on a single modality.

Statistical Analysis and Reporting

Overall model performance for T2-weighted alone, FLAIR alone, and T2+FLAIR models are reported in terms of area under the receiver operating characteristic (AUROC), a metric which accounts for the balance between true positive rate and false positive rate across decision thresholds. AUROC values were also computed for models trained only on age, sex, and CCI. For training data, we applied class-balance resampling, with equal numbers of non-improved and improved patients to reduce class imbalance. After assessing performance on the primary dataset, all models were separately tested on the validation dataset. AUROC values are reported with 95% confidence intervals.

RESULTS
Patient Cohorts

Of 249 patients, 129 (51.8%) were male, 232 (93.2%) were white, and 212 (85.1%) were diagnosed with iNPH (**Table 1**).[6] The distal terminus of the shunt catheter was placed intraperitoneally in 244/249 (98.0%). All patients presented with gait instability with a median estimated gait score of 4/8 (IQR 4-6), 196 (78.7%) presented with urinary incontinence with a median estimated incontinence score of 3/6 (IQR 2-4), and 217 (87.1%) had subjective cognitive impairment (**Table 2**).[1, 2]

Table 1. Patient demographics and characteristics

Patient Characteristic Mean (± SD) or Median (IQR)	Training / Testing (Institution 1, n=249)	Validation (Institution 2, n=33)
Age	74.2 (± 7.5) years	72.1 (± 7.7) years
Sex		
Male	129 (51.8%)	19 (57.6%)
Female	120 (48.2%)	14 (42.4%)
Race		
White	232 (93.2%)	28 (84.8%)
Black/African American	7 (2.8%)	4 (12.1%)
Other/Unknown	10 (4.0%)	1 (3.0%)
BMI	28.5 (± 5.8)	29.1 (±4.6)
CCI	6 (5–7)	4 (3–6)
Shunt laterality		

Right	239 (95.9%)	33 (100%)
Left	10 (4.1%)	0 (0%)
Catheter terminus placement		
Ventriculoperitoneal	244 (98.0%)	33 (100%)
Ventriculopleural	5 (2.0%)	0
NPH Classification		
iNPH	212 (85.1%)	32 (97.0%)
sNPH	37 (14.9%)	1 (3.0%)
Baseline mRS		
0– No symptoms	0	0
1– No significant disability	1 (0.4%)	0
2– Slight disability	107 (43.0%)	8 (24.2%)
3– Moderate disability	83 (33.3%)	8 (24.2%)
4– Moderate-severe disability	41 (16.5%)	15 (45.5%)
5– Severe disability	3 (1.2%)	1 (3.0%)
Unable to Determine	14 (5.6%)	0
8-Point Gait Score	4 (4–6)	5 (4–6)
6-Point Incontinence Score	3 (2–4)	3 (2–4)

The median CCI of the population was 6 (IQR 5-7). Of those who returned for 12-month postoperative follow-up, the greatest overall proportional improvements were observed in gait (70.3%), followed by incontinence (68.0%), overall functional disability (56.4%), and cognition (46.9%). The external validation dataset comprising 33 shunted NPH patients from a second institution overall had similar demographic, symptom, and postoperative improvement distributions (**Tables 1-2**).

Table 2. Presenting symptoms and postoperative improvement; denominators for improvement calculations are patients who had each symptom at baseline and attended follow-up.

Triad of NPH Symptoms + Functional Disability	Present at Baseline (Pre-Op)	Improved at 3 Months Post-Op	Improved at 12 Months Post-Op
Training & Testing Cohort	249/249 (100%)	226/249 (90.8%)	175/249 (70.3%)
Gait Impairment	249 (100%)	165/226 (73.0%)	123/175 (70.3%)
Urinary Incontinence	196 (78.7%)	76/127 (59.8%)	66/97 (68.0%)
Cognitive Impairment	217 (87.1%)	97/208 (46.6%)	75/160 (46.9%)
mRS	—	105/179 (58.7%)	84/149 (56.4%)
Validation Cohort	33/33 (100%)	33/33 (100%)	33/33 (100%)
Gait Impairment	33 (100%)	29/33 (87.9%)	22/33 (66.7%)
Urinary Incontinence	21 (63.6%)	4/33 (12.1%)	3/33 (9.1%)
Cognitive Impairment	31 (93.9%)	14/33 (42.4%)	12/33 (36.4%)
mRS	—	7/33 (21.2%)	6/33 (18.2%)

Machine Learning Models

When trained using T2-weighted imaging alone, the machine learning model achieved AUROC of 0.5125 [0.3392–0.6858] for postoperative improvement in mRS, 0.6994 [0.5901–0.8087] for gait, 0.7304 [0.6253-0.8355] for urinary incontinence, and 0.4479 [0.2763–0.6195] for cognitive impairment (**Table 3**). By contrast, models based on FLAIR imaging were generally better performing, yielding AUROC values of 0.6723 [0.4968-0.8478], 0.7195 [0.6046-0.8344], 0.7929 [0.6912-0.8947], and 0.7175 [0.5533-0.8816], respectively. The combination of T2-weighted and FLAIR sequences offered the best performance in mRS and gait improvement predictions relative to models trained on single-sequence imaging, with AUROC values increasing to 0.7395 [0.5765-0.9024] and 0.8816 [0.8030-0.9602]. Performances when predicting the other outcomes were similar to FLAIR-only models (**Figure 5**). FLAIR-weighted and combined imaging-trained models generally performed better than models trained only on age, sex, and CCI (**Table 3**).

Table 3. Model performances on primary institution dataset; AUROC values represent the results of pre-trained models when evaluated on testing dataset and 95% confidence intervals.

Model Input	mRS Improvement	Gait Improvement	Urinary Improvement	Cognitive Improvement
Age, Sex, CCI	0.6255 [0.5089–0.7421]	0.5413 [0.4205–0.6621]	0.7135 [0.5306–0.8964]	0.6562 [0.4918–0.8207]
T2 Only	0.5125 [0.3392–0.6858]	0.6994 [0.5901–0.8087]	0.7304 [0.6253–0.8355]	0.4479 [0.2763–0.6195]
FLAIR Only	0.6723 [0.4968–0.8478]	0.7195 [0.6046–0.8344]	0.7929 [0.6912–0.8947]	0.7175 [0.5533–0.8816]
T2+FLAIR	0.7395 [0.5765–0.9024]	0.8816 [0.8030–0.9602]	0.7874 [0.6845–0.8903]	0.7230 [0.5600–0.8859]
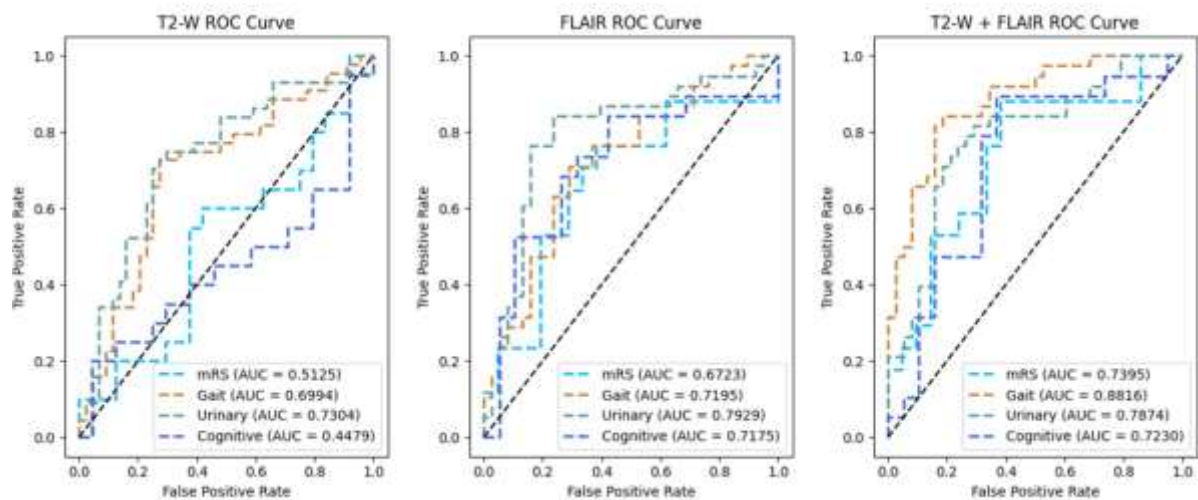
FIG 5. Receiver operating characteristic (ROC) curves demonstrating comparison between models trained on T2-weighted, FLAIR, and both sequences for each of four clinical improvement endpoints on primary institution testing dataset.

When applied to the external validation dataset, T2+FLAIR models were again the best performing for mRS and gait improvements, but similar to single-sequence models for urinary incontinence and cognition (**Table 4**).

Table 4. Model performances on external validation dataset; AUROC values represent the results of the same pre-trained models when evaluated on external validation dataset and 95% confidence intervals.

Model Input	mRS Improvement	Gait Improvement	Urinary Improvement	Cognitive Improvement
T2 Only	0.5513 [0.2874–0.8152]	0.6167 [0.2391–0.9942]	0.7816 [0.4609–1]	0.5732 [0.4326–0.7139]
FLAIR Only	0.7989 [0.6909–0.9068]	0.4758 [0.0517–0.8999]	0.6724 [0.3645–0.9803]	0.6364 [0.5024–0.7703]
T2+FLAIR	0.8291 [0.7271–0.9311]	0.7333 [0.4263–1]	0.7586 [0.4286–1]	0.6310 [0.4326–0.8293]

DISCUSSION

Predicting success of shunt surgery in NPH has been historically challenging. Clinical examination and detailed history taking to identify the NPH symptom triad aids in the diagnosis and selection of surgical candidates, however overall prognostic accuracy rarely exceed 80–85% mainly due to poor negative predictive values of objective CSF dynamic testing methods.[2, 3, 10, 21] Being able to predict the likelihood of improvement of each symptom domain with greater confidence could boost patient-reported quality of life after shunt surgery and aid more individualized decision-making.[22] In this study, we applied a novel AI-driven approach to outcome prediction using two baseline MRI sequences in patients with shunted NPH. Our methods enabled unbiased feature selection from input imaging (**Figure 2**) and optimization of outcome prediction across a broader space of potential features relative to standard statistical outcome prediction methods (e.g., regression). Our sizable primary study cohort included both iNPH and sNPH patients diagnosed clinically (**Table 1**), not dependent on lumbar tap test results.[21] We observed postoperative improvement rates across the NPH triad similar to the reported literature (**Table 2**).[8, 23] In this setting, we hypothesized that MRI-based predictive models achieve optimized performance when combining T2-weighted and FLAIR MRI sequences, each containing clinically useful features of the underlying disease, though this complementarity may pertain to some symptom domains but not others.

Our findings confirm the hypothesis, demonstrating proof-of-concept that machine learning models trained on both FLAIR and T2-weighted sequences showed improved prediction of treatment success (**Table 3**). These results confirm the complementary "power" of combining features from multiple sequences into a single model: while overall performance in terms of AUROC was generally less impressive for T2-weighted imaging alone, values increased substantially across mRS and gait outcome domains for the combined (T2+FLAIR) model, and for urinary and cognitive improvement when applying either the FLAIR-only or combined models (**Table 3**). The optimal model performances for predicting improvement in gait (AUROC=0.88 [0.80–0.96]), cognition (AUROC=0.72 [0.56–0.89]), and overall function (AUROC=0.74 [0.57–0.90]) were observed when applying the T2+FLAIR model, while the maximum performance for predicting urinary symptom improvement was seen with the FLAIR-only model 0.79 [0.69–0.89]. While the T2-weighted sequence offers more detailed information about CSF and subarachnoid space volumes, FLAIR provides information about transependymal flow and white matter change associated with parenchymal volume loss. Though it is possible automatically extracted radiomic features associated with these specific differences between the two sequences led to the observed performance differences across symptom domains between T2, FLAIR, and T2+FLAIR models, the methods do not enable us to readily interpret the extracted features in order to confirm or refute this theory.

Though our methods and results do not define or focus on any individual radiomic feature explicitly, our approach is supported by prior studies which have used more traditional statistical approaches to investigate the value of several structural and CSF space-related imaging features for diagnosis and/or prognosis of NPH.[11, 17, 18, 24, 25] MRI-based disproportionately enlarged subarachnoid space hydrocephalus (DESH) score has been found to be statistically disparate between patients who improve versus those who don't across some clinical symptom metrics.[16, 24] Further, these findings build upon recent studies by *Shao et al.* and others who applied machine learning approaches to capture features of the ventricular system and differentiate NPH patients from non-NPH control individuals,[26-28] and *Tsou et al* who demonstrated a convolutional neural network approach to measuring aqueductal CSF flow from phase-contrast MRI.[29] In our study, we employed an automated radiomic feature extraction and outcome prediction pipeline which was at least as predictive of symptom improvement across multiple domains as these previously reported approaches. Our approach also did not require radiologic interpretation or measurement of multiple metrics as the DESH score requires.

Additionally, we define an analytic framework for comparing single-sequence versus multi-sequence models for outcome

prediction. While model performance improved by combining T2 and FLAIR when predicting mRS and gait improvements, performance was similar between T2+FLAIR and FLAIR-only trained-models when predicting urinary and cognitive symptom improvement. Taken together, these findings suggest that T2-weighted imaging may not provide additional features useful for predicting these outcomes, while features available on T2-weighted sequences are more sensitive to CSF space and cerebral blood flow characteristics thought to impact gait-related function.[30] Importantly, overall function as evaluated by mRS is more dependent on gait and less dependent on the cognition and urinary incontinence, given the inclusion of mobility-related function explicitly in the score.[8, 31]

Further work is needed to understand why some imaging studies, and some specifically identified features within them, may hold more prognostic relevance than others, given overall limited knowledge of the underlying disease mechanisms of NPH. It is our hope that this study will lay the groundwork for a more sophisticated future predictive model which integrates all available data of known prognostic importance. We believe this is among the most comprehensive imaging-based demonstrations of NPH shunt outcome prediction to date, benefitting from an unbiased approach not tethered to any specific hypothesis about individually selected features, as prior studies largely have been.

Comparison with External Validation Dataset

To improve the rigor of our analysis and assess generalizability to external NPH cohorts, we applied our models to an independent NPH population from a second institution. In validation analyses, high performances for predicting mRS, gait, and urinary symptom improvements were maintained, but we observed a drop in performance when predicting cognitive improvement (**Table 4**). Surprisingly, predictions of improvement in overall function (mRS) with either the FLAIR-only or T2+FLAIR models were even better in the validation cohort, with AUROC values of 0.80 [0.69–0.91] and 0.83 [0.73–0.93], respectively.

The external validation dataset was different from the primary dataset in two important respects: the lower proportion of sNPH patients and the lower rate of improvement across symptom domains. While retrospectively estimated clinical outcomes related to gait and urinary incontinence may be more readily evaluated in the absence of detailed prospective study-specific assessments, cognitive improvement is more difficult to objectively assess in this manner. This may explain the poor performance of the cognitive improvement prediction model on the validation cohort. Furthermore, the confidence intervals of the estimated AUROC value estimates were quite broad, likely owing to the small sample size (Table 4, n=33). Confidence intervals were narrower for model evaluation using the primary dataset testing split (Table 3, n=55–60, depending on the model). Accordingly, while limited statistical conclusions that can be drawn from comparing model performances without a much larger sample size, the overall performance of the generated models on both the primary testing and external validation datasets provides conceptual evidence that machine learning models trained on multi-sequence imaging data may comprise a generalizable approach to improved clinical outcome prediction in NPH. Inclusion of both iNPH and sNPH subpopulations within our cohorts further lends generalizability, as sNPH patients are often excluded from NPH outcome studies and might be expected to present with more heterogeneous imaging features on MRI. Future work might also seek to leverage additional layers of patient data, such as clinical biomarker data obtained from cerebrospinal fluid, which has also recently been shown to offer clinically useful outcome prediction performance.[32, 33]

Comparison with Other Models

Within our cohort, models trained on demographic data and CCI without imaging had poor predictive value, underscoring the added value of neuroimaging features which cannot be captured by clinical data alone. Several studies examining correlations between comorbidity data and outcome in NPH have also documented poor prediction based on comorbidity metrics alone.[13, 34, 35] The limitations of existing predictive tools are particularly apparent when NPH is present alongside Parkinson's and/or Alzheimer's diseases.[36, 37] Multi-sequence imaging models such as the T2+FLAIR model presented in this study could be further developed to incorporate T1-weighted imaging more sensitive to cognitive outcome,[37] as well as other sequences (e.g., diffusion weighted imaging). Future research is needed to determine the practical value of incorporating these additional sequences not investigated in the present study, but it is certainly plausible that incorporating T1- or diffusion-weighted sequences could improve model performance in outcome prediction domains where our T2+FLAIR model is weakest (e.g., cognition). Further, outcome prediction models might endeavor to capture more detailed systemic and neurodegenerative comorbidity information than previously published studies of comorbidity burden and NPH outcome,[13-15] given the possibility that such clinical data could also further enhance the performance of models based on imaging alone.

Limitations

While we present the first fully integrated AI model trained on multiple MRI sequences, we selected T2-weighted and FLAIR imaging based on availability through routine clinical practice. Not considered were other sequences such as T1- or diffusion-weighted sequences which

has previously been shown to be of potential importance in NPH owing to the retrospective methods of this study.[18, 37] While imaging acquisition was generally uniform over the study inclusion period, given that the majority of scans were acquired at a single academic medical center under the same protocol, the minority of patients whose imaging originated from outside centers were not excluded on that basis alone. Accordingly, some heterogeneity in acquisition MR acquisition parameters likely exists, though pre-processing pipeline was intended to partially mitigate any such effect.

We retrospectively abstracted clinical data including gait and continence scores, improvement in symptoms, and mRS from the treating surgeon's clinical documentation, and a portion of patients were lost to follow-up. Given nearly 30% loss to follow-up rate at 12-months post-op (versus only 10% at 3-month), the 3-month follow-up was utilized for retrospective outcome assessment for a subset of cases (approximately 20%). While standardized scales were used to estimate impairment scores in the gait and incontinence domains, cognitive impairment was assessed less objectively. Future studies would benefit from standardized implementation of quantitative cognition metrics such as mini mental status examination (MMSE).

Finally, while we hypothesized that some of the intuitively observable differences between T2 and FLAIR sequences (e.g., transependymal flow on FLAIR) might give rise to their additive value in a combined model, the AI methods utilized do not give us ready access to the automatically identified radiomic features used in predictive modeling, hence this mechanistic aspect of the hypothesis remains unanswered by the present study.

CONCLUSIONS

AI algorithms leveraging combined imaging features from preoperative T2-weighted and FLAIR sequences were generally more predictive of postoperative shunt outcome in NPH than models built using one of these sequences. Models performed best for prediction of gait and incontinence improvement, and slightly worse for predicting improvement in mRS and cognition.

REFERENCES

1.   Hellström P, Klinge P, Tans J, et al. A new scale for assessment of severity and outcome in iNPH. *Acta Neurol Scand* 2012;126:229-237
2.   Klinge P, Hellström P, Tans J, et al. One-year outcome in the European multicentre study on iNPH. *Acta Neurol Scand* 2012;126:145-153
3.   Relkin N, Marmarou A, Klinge P, et al. Diagnosing idiopathic normal-pressure hydrocephalus. *Neurosurgery* 2005;57:S4-16; discussion ii-v
4.   Bradley WG, Jr. CSF Flow in the Brain in the Context of Normal Pressure Hydrocephalus. *AJNR Am J Neuroradiol* 2015;36:831-838
5.   Rigamonti D, Yasar S, Vivas-Buitrago T, et al. Letter to Our Colleagues Family Practitioners, Geriatricians, and Radiologists to Increase Awareness Regarding Idiopathic Normal Pressure Hydrocephalus. *World Neurosurg* 2023
6.   Daou B, Klinge P, Tjoumakaris S, et al. Revisiting secondary normal pressure hydrocephalus: does it exist? A review. *Neurosurg Focus* 2016;41:E6
7.   Alvi MA, Brown D, Yolcu Y, et al. Prevalence and Trends in Management of Idiopathic Normal Pressure Hydrocephalus in the United States: Insights from the National Inpatient Sample. *World Neurosurg* 2021;145:e38-e52
8.   Giordan E, Palandri G, Lanzino G, et al. Outcomes and complications of different surgical treatments for idiopathic normal pressure hydrocephalus: a systematic review and meta-analysis. *J Neurosurg* 2018:1-13
9.   El Ahmadieh TY, Wu EM, Kafka B, et al. Lumbar drain trial outcomes of normal pressure hydrocephalus: a single-center experience of 254 patients. *J Neurosurg* 2019;132:306-312
10.   Ishikawa M, Hashimoto M, Mori E, et al. The value of the cerebrospinal fluid tap test for predicting shunt effectiveness in idiopathic normal pressure hydrocephalus. *Fluids Barriers CNS* 2012;9:1
11.   Lotan E, Damadian BE, Rusinek H, et al. Quantitative imaging features predict spinal tap response in normal pressure hydrocephalus. *Neuroradiology* 2022;64:473-481
12.   Rydja J, Eleftheriou A, Lundin F. Evaluating the cerebrospinal fluid tap test with the Hellström iNPH scale for patients with idiopathic normal pressure hydrocephalus. *Fluids Barriers CNS* 2021;18:18
13.   Israelsson H, Larsson J, Eklund A, et al. Risk factors, comorbidities, quality of life, and complications after surgery in idiopathic normal pressure hydrocephalus: review of the INPH-CRasH study. *Neurosurg Focus* 2020;49:E8
14.   Klinge PM, Ma KL, Leary OP, et al. Charlson comorbidity index applied to shunted idiopathic normal pressure hydrocephalus. *Sci Rep* 2023;13:5111
15.   Pyykkö OT, Nerg O, Niskasaari HM, et al. Incidence, Comorbidities, and Mortality in Idiopathic Normal Pressure Hydrocephalus. *World Neurosurg* 2018;112:e624-e631
16.   Skalický P, Vlasák A, Mládek A, et al. Role of DESH, callosal angle and cingulate sulcus sign in prediction of gait responsiveness after shunting in iNPH patients. *J Clin Neurosci* 2021;83:99-107
17.   Thavarajasingam SG, El-Khatib M, Vemulapalli K, et al. Radiological predictors of shunt response in the diagnosis and treatment of idiopathic normal pressure hydrocephalus: a systematic review and meta-analysis. *Acta Neurochir (Wien)* 2023;165:369-419
18.   Reiss-Zimmermann M, Scheel M, Dengl M, et al. The influence of lumbar spinal drainage on diffusion parameters in patients with suspected normal pressure hydrocephalus using 3T MRI. *Acta Radiol* 2014;55:622-630
19.   van Swieten JC, Koudstaal PJ, Visser MC, et al. Interobserver agreement for the assessment of handicap in stroke patients. *Stroke* 1988;19:604-607
20.   Feng X, Tustison NJ, Patel SH, et al. Brain Tumor Segmentation Using an Ensemble of 3D U-Nets and Overall Survival Prediction Using Radiomic Features. *Front Comput Neurosci* 2020;14:25
21.   Marmarou A, Bergsneider M, Klinge P, et al. The value of supplemental prognostic tests for the preoperative assessment of idiopathic normal-pressure hydrocephalus. *Neurosurgery* 2005;57:S17-28; discussion ii-v
22.   Hallqvist C, Grönstedt H, Arvidsson L. Gait, falls, cognitive function, and health-related quality of life after shunt-treated idiopathic normal pressure hydrocephalus-a single-center study. *Acta Neurochir (Wien)* 2022;164:2367-2373
23.   Tullberg M, Persson J, Petersen J, et al. Shunt surgery in idiopathic normal pressure hydrocephalus is cost-effective-a cost utility analysis. *Acta Neurochir (Wien)* 2018;160:509-518
24.   Shinoda N, Hirai O, Hori S, et al. Utility of MRI-based disproportionately enlarged subarachnoid space hydrocephalus scoring for predicting prognosis after surgery for idiopathic normal pressure hydrocephalus: clinical research. *J Neurosurg* 2017;127:1436-1442

25.	Kockum K, Lilja-Lund O, Larsson EM, et al. The idiopathic normal-pressure hydrocephalus Radscale: a radiological scale for structured evaluation. *Eur J Neurol* 2018;25:569-576

26.	Shao M, Han S, Carass A, et al. Brain ventricle parcellation using a deep neural network: Application to patients with ventriculomegaly. *Neuroimage Clin* 2019;23:101871

27.	Rau A, Kim S, Yang S, et al. SVM-Based Normal Pressure Hydrocephalus Detection. *Clin Neuroradiol* 2021;31:1029-1035

28.	Zhou X, Ye Q, Yang X, et al. AI-based medical e-diagnosis for fast and automatic ventricular volume measurement in patients with normal pressure hydrocephalus. *Neural Comput Appl* 2022:1-10

29.	Tsou CH, Cheng YC, Huang CY, et al. Using deep learning convolutional neural networks to automatically perform cerebral aqueduct CSF flow analysis. *J Clin Neurosci* 2021;90:60-67

30.	Klinge PM, Brooks DJ, Samii A, et al. Correlates of local cerebral blood flow (CBF) in normal pressure hydrocephalus patients before and after shunting--A retrospective analysis of [(15)O]H(2)O PET-CBF studies in 65 patients. *Clin Neurol Neurosurg* 2008;110:369-375

31.	Quinn TJ, Dawson J, Walters MR, et al. Functional outcome measures in contemporary stroke trials. *Int J Stroke* 2009;4:200-205

32.	Grønning R, Jeppsson A, Hellström P, et al. Association between ventricular CSF biomarkers and outcome after shunt surgery in idiopathic normal pressure hydrocephalus. *Fluids Barriers CNS* 2023;20:77

33.	Levin Z, Leary OP, Mora V, et al. Cerebrospinal fluid transcripts may predict shunt surgery responses in normal pressure hydrocephalus. *Brain* 2023;146:3747-3759

34.	Valsecchi N, Mantovani P, Piserchia VA, et al. The Role of Simultaneous Medical Conditions in Idiopathic Normal Pressure Hydrocephalus. *World Neurosurg* 2022;157:e29-e39

35.	Koo AB, Elsamadicy AA, Renedo D, et al. Hospital Frailty Risk Score Predicts Adverse Events and Readmission Following a Ventriculoperitoneal Shunt Surgery for Normal Pressure Hydrocephalus. *World Neurosurg* 2023;170:e9-e20

36.	Davis A, Gulyani S, Manthripragada L, et al. Evaluation of the effect comorbid Parkinson syndrome on normal pressure hydrocephalus assessment. *Clin Neurol Neurosurg* 2021;207:106810

37.	Giannakopoulos P, Montandon ML, Herrmann FR, et al. Alzheimer resemblance atrophy index, BrainAGE, and normal pressure hydrocephalus score in the prediction of subtle cognitive decline: added value compared to existing MR imaging markers. *Eur Radiol* 2022;32:7833-7842